RSC Advances

ROYAL SOCIETY OF CHEMISTRY

www.rsc.org/advances

An electrochemical chiral sensor of tryptophan enantiomers based on reduced graphene oxide/1,10-phenanthroline copper(II) functionnal composites

Hao Gou[a], Jingxian He[b], Zunli Mo[a*], Xiaojiao Wei[a], Rere Hu[a] and Yawei Wang[a]

[a] *Key Laboratory of Eco-Environment-Related Polymer Materials, Ministry of Education of China, and Key Laboratory of Polymer Materials of Gansu Province, College of Chemistry and Chemical Engineering, Northwest Normal University, Lanzhou 730070, PR China.*

[b] *School of Chemistry and Environmental Science, Lanzhou City University, Lanzhou 730070, PR China.*

Abstract

An electrochemical chiral sensor based on 1,10-phenanthroline copper(II) (PhenCu) complex non-covalent functionalize reduced graphene oxide (RGO) has been developed for electrochemical discrimination of tryptophan (Trp) enantiomers. The formation and morphology of reduced graphene oxide/1,10-phenanthroline copper(II) (RGO/PhenCu) composites were confirmed by Fourier-transform infrared spectra (FT-IR) and scanning electron microscopy (SEM). Cyclic voltammetry (CV) was employed to monitor the electrochemical behavior when RGO/PhenCu simply modified on glassy carbon electrode (RGO/PhenCu/GCE). The reduction of peak current was significantly different when the chiral sensor interacted with L-Trp and D-Trp. It suggested that the RGO/PhenCu/GCE can be used as an electrochemical chiral sensor for the discrimination of Trp enantiomers. Further study showed that the peak currents were linearly decreased along with an increasing percentage of L-Trp of Trp racemic mixture. The RGO/PhenCu/GCE electrochemical chiral sensor with rapid recognition, good sensitivity and high stability provided an efficient method to recognize and determine Trp enantiomers.

Keywords: Electrochemical chiral sensor; Enantioselectivity recognition; Reduced Graphene Oxide; PhenCu; Tryptophan enantiomers

1. Introduction

Chiral sensors are important from the viewpoint of medical care and pharmaceutical

Corresponding author at: College of Chemistry and Chemical Engineering, Northwest Normal University, Lanzhou 730070, PR China.
E-mail address: nwnumozl@163.com.

technologies because most biologically relevant molecules possess chirality and chiral molecules.[1,2] However, the performance of the enantiomers of these chiral molecules often exhibits remarkable discrepancy in terms of biochemical activity, toxicity, potency, pathways of metabolism and so on.[3] Nowadays, chiral discriminate of biological molecules, such as carbohydrates, peptides and amino acids, has attracted increasing interest in the biochemical and pharmaceutical fields.[4-6] The traditional discriminate enantiomers techniques are usually based on high performance liquid chromatography, chemoluminescence and capillary electrochromatography.[7] Although the reported techniques are useful for the determination of enantiomeric purity, these are not only require expensive chiral columns and require complex sample pretreatment, but also many of them have indicated no difference between two enantiomeric forms of some amino acids.[8] In comparison, electrochemical methods can be evaluated as potential enantiomeric analysis techniques due to their advantages in high stability and sensitivity, low cost, and rapid detection.[9]

Tryptophan enantiomers, which have the asymmetric carbon in their structure, play a very important role in the biological system. As an essential amino acid, Trp has been determined to be a precursor of the neurotransmitter serotonin, and the level of Trp in plasma is closely related to the extent of hepatic disease.[10] Therefore, it is very important to develop an alternative method for chiral discriminate of Trp enantiomers to meet both general and practical challenges. Several strategies concerning the discriminate of enantiomeric pair of Trp, including a time resolved fluorescence technique,[11] potential-induced technique[12] and electrode column technology.[13] Despite these tremendous achievements, the realization of low-cost, facile and sensitive recognition of enantiomers of Trp is still challenging.

Graphene, a single layer of sp^2 bonded carbon atoms in a honeycomb two-dimensional lattice, has attracted intense interest as electrochemical sensing materials owing to its extraordinary physical and chemical properties.[14] In the meantime, noticeable progress also has been made in the utilization of graphene-based composites towards applications in electrochemical analysis. For example, a graphene/Pt-modified glassy carbon electrode was created to simultaneously characterize ascorbic acid, dopamine, and uric acid levels.[15] Deng et al. developed a novel 1,4-bis (4-aminophenylethynyl)benzene/graphene nanocomposite modified electrode to successfully demonstrated for dopamine determination in human serum samples.[16] Wu et al. synthesized a new

type of porphyrin-functionalized graphene and used for highly selective and sensitive detection of dopamine.[17] Recently, Asadi et al. produced a graphene nanoribbon/polyaniline composite film application in electrochemical determination of dobutamine and it shows impressive performance.[18] Thus it can be seen that graphene-based materials have been used in electrochemical sensors and biosensors. And graphene layer immobilized on the electrode surface that not only provides an effective sensing platform but also separates the analytical signal.[8] To the best of our knowledge, however, there is still a little study has been done on the application of graphene, especially modified graphene with selective materials to form a functional composite in electrochemical detection of chiral molecules.

Herein, a novel and stable reduced graphene oxide/1,10-phenanthroline copper(II) functional composites were first synthesized based on the self-assembly of through non-covalent interactions. Non-covalent modifications of graphene will not destroy graphene's intrinsic structure, thus its excellent properties can be preserved. Via non-covalent interactions to afford varied functional composite materials with enhanced mechanical properties, tunable electrical conductivity and potential applications for solar cells, electronics devices and sensing.[19] Under the non-covalent interaction model, the aromatic ring of reactants is inclined to be parallel and close to the sp^2 network of graphene, and this reaction are easy to achieve.[20] And we found that the PhenCu needle-like structures are uniformly distributed on the surface of reduced graphene oxide and formed the graphene-based composites, which makes it have potential application in various fields. The composites shown good capacitive performance and excellent chiral recognition performance when it was simply modified on GCE. The stepwise fabrication process is illustrated schematically in Scheme 1. In addition, the RGO/PhenCu composites adhere well to glassy carbon electrode surfaces by dispersion of powder in absolute ethanol. This process don't need any adhesive like the nafion, and this makes the electrochemical chiral sensor is more economic and environmentally friendly. Since the coordination capacity of Trp enantiomers and 1,10-phenanthroline is different, highly sensitive and selective electrochemical discrimination of Trp enantiomers was realized via ligand exchange. Moreover, the enantioselectivity of the RGO/PhenCu/GCE was systematically discussed by incubation time and pH. The reduced graphene oxide/1,10-phenanthroline copper(II) functional composites may provide an alternative way for the design of novel electrochemical chiral sensor with superior performances.

2. Experimental

2.1 Preparation of 1,10-phenanthroline copper(II)

Methyl alcohol was added to distilled water (1:1v/v) to form mixed solution. 1,10-phenanthroline (50 mM) and $CuCl_2 \cdot 2H_2O$ (50 mM) were dropped into the above solution stirred at room temperature for 30 min. The blue solution gradually turned to blue-green, and becoming cloudy. The solution was filtered and washed 3 to 4 times with distilled water. The resulting blue-green solid was dried at 60 °C for 12 h to produce the PhenCu.

2.2 Synthesis of RGO/PhenCu

Graphite oxide (GO) was synthesized from graphite powder by the improved method,[21] and reduced graphene oxide was obtained by reduction of GO. The RGO/PhenCu was prepared by the following method: 0.02g of RGO was exfoliated in 100 mL of absolute alcohol with ultrasonic treatment for 1 h to form a black solution. PhenCu (0.06g) was dropped into the RGO solution and stirred at 30 °C for 24 h. The obtained composites were filtered and adequately washed with water and absolute alcohol several times, and dried at 50 °C for 24 h.

2.3 Preparation of the RGO/PhenCu/GCE chiral sensor as working electrode

The surface of GCE was polished carefully with 1.0, 0.3 and 0.05 μm alumina slurry in turn, and rinsed with doubly distilled water, followed cleaned by sonication in ethanol solution and doubly distilled water successively and dried in the air.

The RGO/PhenCu composites (1mg/mL) were dispersed into absolute alcohol and sonicated for 30 min. Then a drop of suspension (5 μL) was cast onto the freshly polished GCE and then dried in air at room temperature.

2.4 Reagents and apparatus

All chemicals were of analytical grade and used without further purification. Graphite powder (99.99%), L-Trp, D-Trp and 1,10-phenanthroline were obtained from Aladdin Industrial Corporation. Concentrated H_2SO_4, H_2O_2, $KMnO_4$, $K_3[Fe(CN)_6]$, $K_4[Fe(CN)_6] \cdot 3H_2O$ was supplied by Tianjin Kaixin Chemical reagents Co., Ltd. $NaH_2PO_4 \cdot 2H_2O$, $Na_2HPO_4 \cdot 12H_2O$, KNO_3, $CuCl_2 \cdot 2H_2O$ were purchased from Tianjin kaitong Chemical Plant reagents Co., Ltd.

The scanning electron microscopy image was obtained by JSM-6701F cold field emission scanning electron microscope (Japan). Fourier-transform infrared spectra were recorded on an EQUINOX55 FT-IR spectrometer with KBr pellets. Cyclic voltammetry (CV) measurements was

performed with a CHI 660E electrochemistry workstation (Shanghai Chenhua Instruments Co., China).

2.5 Experimental measurements

All electrochemical experiments were carried out with a three-electrode system, in which either the bare or modified glassy carbon electrode was used as the working electrode, a saturated calomel electrode was used as the reference electrode and a platinum wire was used as the auxiliary electrode. The CV scan was carried out from 0.2 to 0.6 V at a rate of 50 mV s^{-1} in 5 mM $[Fe(CN)_6]^{4-/3-}$ solution with various pH were prepared with phosphate buffer solutions (PBS) using 0.1 M KNO_3 as the supporting electrolyte.

The detection was based on the differences of oxidation peak current (ΔI) before and after the RGO/PhenCu/GCE chiral sensor was immersed into a 5 mM L-Trp or D-Trp solution. So the ΔI was calculated by using the equation: $\Delta I = I_0 - I_1$, the I_0 was the oxidation peak current of RGO/PhenCu/GCE chiral sensor, and I_1 was the oxidation peak current after the chiral sensor had interacted with the Trp enantiomer solutions. $\Delta I' = I_0' - I_1'$, I_0' was the oxidation peak current after the chiral sensor had interacted with the D-Trp, I_1' was the oxidation peak current after the chiral sensor had interacted with the L-Trp.

3. Results and discussion

3.1 Characterization of the composites

Fig. 1 show the Fourier-transform infrared spectra of Phen, PhenCu, reduced graphene oxide, and the RGO/PhenCu composites. Compared with the FTIR spectrum of the Phen (Fig. 1a), in spectrum of PhenCu (Fig. 1b), the characteristic peaks of 1,10-phenanthroline showed up , especially the peaks at 1523 cm^{-1}, 867 cm^{-1}, 717 cm^{-1} are red-shifted after forming the PhenCu. In addition, all the characteristic peaks become weaker. From the above analysis, it indicates coordination of Cu^{2+} and the 1,10-phenanthroline. As shown in Fig. 1b, c and d, the FTIR spectrum of RGO/PhenCu composites exhibits their respective absorption features of RGO and PhenCu, and the peaks become weak and shifted. The result confirms that the PhenCu has been non-covalently grafted onto the surface of the reduced graphene oxide sheet successfully.

Reduced graphene oxide is modified non-covalently by PhenCu, which can be further confirmed by scanning electron microscopy. As can be seen in Fig. 2a, the reduced graphene oxide appeared to be of good quality with large sizes and thickness. And the surface is glazed and

wrinkled, look to resemble silks and satins. In Fig. 2b, the morphology of the RGO/PhenCu composites have a substantial difference from that of reduced graphene oxide, it can be clearly seen that the PhenCu needle-like structures are uniformly distributed on the surface of reduced graphene oxide and formed the reduced graphene oxide-based composites. Large-scale SEM image showed that the sizes of the PhenCu needle-like structures are about 1–2 μm (Fig. 2c). Nevertheless, The PhenCu complex eventually become amorphous structures after grown naturally 3 months without any processing, as shown in Fig. 2d. In contrast, the RGO/PhenCu composites have become more orderly, this may be because reduced graphene oxide provide a sound basis for growth of PhenCu complex. On the other hand, the PhenCu complex can also grow by itself due to there are force among1,10-phenanthroline ligands. The complex grows along the pros and cons of reduced graphene oxide into needle-like structures, and the erect part looks like peeled pomelo. This structure gives two advantages: the one is increasing the contact area between the composites and enantiomers which could promote the coordination reaction, the other is that reduced graphene oxide provide an effective sensing platform and greatly improve the detection sensitivity of chiral tryptophan.

3.2 Electrochemical characterization of the composites

We studied the electrochemical and sensing performance of the RGO/PhenCu composites by cyclic voltammetry and galvanostatic charge-discharge test. Fig. 3a shows CV curves of SCE, RGO/PhenCu composites at a scan rate of 50 mV s^{-1}. The integral area of RGO/PhenCu composites is much bigger than that of SCE. And the CV curves of the composites shows a well-defined redox peaks at around 0.2V, which indicating the redox reaction have a good reversibility and a fast charge transfer process. Fig. 3b shows galvanostatic discharge curves of RGO/PhenCu composites at 1 A g^{-1}. Through the calculation, the specific capacitance is 362 F g^{-1} at the current density of 1 A g^{-1}, which is higher than pure reduced graphene oxide. It is worthy of mentioning that the charge/discharge curves are very symmetrical and an obvious plateau at low potentials can be observed. The plateau is related to the quick Faradaic reactions from RGO/PhenCu composites, which is in agreement with the CV curves. The cycle durability is an important concern for capacitor. As seen in Fig. 3c, after 200 cycles at 50 mV s^{-1}, the curve remained nearly unchanged, indicating excellent electrochemical stability of RGO/PhenCu composites. This study basically showed that RGO/PhenCu composites is expected to be a

supercapacitors.

3.3 Enantioselective discrimination of Trp enantiomers

More importantly, the electrochemical response before and after the RGO/PhenCu/GCE interacted with L-Trp and D-Trp has been investigated by CV. As it can be seen clearly in Fig. 3a, the peak current decreased after the chiral sensor was dipped in 5 mM Trp enantiomers solution for 6 min. However, an obvious chiral discrepancy was noticed, where the larger decrease was obtained from RGO/PhenCu/GCE and L-Trp (the current declined to 16.06 A g^{-1}) than that of RGO/PhenCu/GCE and D-Trp (the current declined to 7.16 A g^{-1}). That is, the total amount of chiral ligand exchange existed between RGO/PhenCu and L-Trp was larger than D-Trp. The main reaction is described as follows:

$$\text{L-Trp} + [\text{Cu(II)(Phen)}_2] = [\text{(L-Trp)Cu(II)(Phen)}] + \text{Phen}$$

$$\text{D-Trp} + [\text{Cu(II)(Phen)}_2] = [\text{(D- Trp)Cu(II)(Phen)}] + \text{Phen}$$

That is to say, coordination capacity of Trp enantiomers and Cu(II) is stronger than that of Phen, and L-Trp can exchange one Phen to form [(L-Trp)Cu(II)(Phen)] more easy. In this reaction process, the perfectly ordered needle-like structure of RGO/PhenCu composites can increase the contact area between PhenCu and Trp enantiomers which is conducive to accelerate the chiral ligand exchange speed, thus shortening the measurement time and improving sensing test efficiency. Therefore, RGO/PhenCu/GCE could discriminate between the Trp enantiomers.

3.4 the influence of the amount of Trp enantiomers

In order to gain an insight to the relationship between the peak current and the concentration of Trp and best testing concentration of Trp enantiomers, additional CV measurements were performed in the presence of different concentrations of D-Trp and L-Trp. We found that the peak current of D-Trp decreased with the increasing of D-Trp in the range of 3–6 mM in Fig.4a. But the reduction of peak current from 3 mM to 5 mM is slow and uniform. This change become bigger when D-Trp concentration increase to 6mM. It is mainly because only small amounts of D-Trp can react with PhenCu, and the effective concentration of $[Fe(CN)_6]^{4-/3-}$ has fallen after adding the D-Trp. The peak current of L-Trp also decreased with increasing of L-Trp concentrations in the range of 3–6 mM as shown in Fig. 4b. It is important to note that although the D-Trp and L-Trp show decrease with increasing of Trp enantiomers concentrations, the L-Trp gives more obvious change than the D-Trp. It really shows that a larger amount of L-Trp exhibit ligand exchange reaction with PhenCu. It also means that L-Trp has a stronger affinity to PhenCu than D-Trp does. Besides, as shown in Fig. 4c, $\Delta I'$ had the highest when the concentration of Trp enantiomers is 5

mM. This shows that it can maximize react with L-Trp when the content of RGO/PhenCu on the GCE is kept constant. Therefore, 5 mM was chosen as testing concentration.

3.5 the influence of interaction time

The influence of reaction time for the enantioselective interaction was researched between 30s and 12 min. As shown in Fig. 5, the peak currents decreased with prolongation of the reaction time. The decrease is not evidence after 6 min whether L-Trp or D-Trp. And the ΔI had maintained maximum after the interaction time was increased to 6 min. So, 6 min was adopted as the best recognition time in this work. This value is smaller than previously reported,[22-24] which raises the detecting efficiency significantly.

3.6 the influence of pH

The influence of pH to the enantioselective discrimination was investigated at pH range from 5.3 to 7.0 (Fig. 6). However, we find that the ΔI was smaller after PBS addition. It can be seen that the maximum difference of peak current density appeared without PBS. The reason may be that the addition of PBS depressed ligand exchanging reaction between RGO/PhenCu/GCE and Trp enantiomers. Therefore, all subsequent experiments were performed without PBS.

3.7 Application of the chiral sensor

The RGO/PhenCu/GCE was also used to detect the current responses of Trp enantiomeric mixtures at different fixed ratios. The standard calibration curves and cyclic voltammograms of Trp enantiomeric mixtures are presented in Fig. 7. It was clear that the peak currents were uniformly decreased along with the increasing amount of L-Trp. Moreover, the correlation between ΔI and L-Trp% exhibited a linear relationship. The linear regression was expressed as $\Delta I = 0.09171 \times \text{L-Trp\%} + 7.04443$ ($R^2 = 0.99268$). To the best of our knowledge, such good chiral recognition ability is comparable or superior to the best results reported in the literature as shown in Table 1. By comparison, this electrochemical chiral sensor is more convenient, high-efficiency and sensitive. These results demonstrated that the RGO/PhenCu/GCE electrode gives an opportunity for not only higher chiral recognition ability to Trp enantiomeric mixtures but also provides the determination one enantiomer in the presence of the counter isomer.

4. Conclusion

In summary, a novel PhenCu functionalized reduced graphene oxide composites were successfully synthesized. And the composites possess distinctive needle-like structures, which

makes it have potential application in various fields. For example, it has good capacitive performance. More importantly, the RGO/PhenCu composites have been fabricated for discrimination of Trp enantiomers when it was simply modified on GCE. Reduced graphene oxide with high electron mobility and large surface area immobilized on GCE has been expected not only for providing an effective sensing platform but also for improving the detection sensitivity. And this special structure would be more helpful for increasing the contact area between the composites and enantiomers. Therefore, the RGO/PhenCu/GCE chiral sensor with high sensitivity and rapid detection has been developed to recognize Trp enantiomers by ligand exchange. Moreover, the chiral sensor is very simple, convenient, economical and highly efficient. This study could promote an understanding of competitive reaction between coordination compound. Besides, it also provides a simple and efficient method to discriminate various chiral enantiomers via electrochemical reactions.

Acknowledgements

The authors would like to thank the financial support the National Natural Science Foundation of China (51262027), the Natural Science Foundation of Gansu Province (0803RJZA009), Science and Technology Tackle Key Problem Item of Gansu Province (2GS064-A52-036-08) and Gansu Key Laboratory of Polymer Materials (ZD-04-14), and supported by the fund of the State Key Laboratory of Solidification Processing in NWPU (SKLSP201011).

References

1 Y. F. Bu, S. Wang, Q. Chen, H. L. Jin, J. J. Lin and J. C. Wang, *Electrochemistry Communications*, 2012, **16,** 80–83.

2 M. Trojanowicz, *Electrochemistry Communications*, 2014, **38,** 47–52.

3 L. Zhang, C. L. Xu, C. W. Liu and B. X. Li, *Analytica Chimica Acta*, 2014, **809,** 123–127.

4 B. M. Wei, N. N. Liu, J. T. Zhang, X. W. Ou, R. X. Duan, Z. K. Yang, X. D. Lou and F. Xia, *Analytical Chemistry*, 2015, **87,** 2058−2062.

5 L. Taujenis, V. Olšauskaitě and A. Padarauskas, *Journal of Agricultural and Food Chemistry*, 2014, **62,** 11099−11108.

6 R. F. Tiphaine, A. Nathalie, G. Laurence, J. F. Goossens and C. Danel, *Carbohydrate Polymers*, 2015, **115,** 598–604.

7 M. Li, X. Liu, F. Y. Jiang, L. P. Guo and L. Yang, *Journal of Chromatography A*, 2011, **1218,** 3725–3729.

8 E. Zor, I. H. Patir, H. Bingol and M. Ersoz, *Biosensors and Bioelectronics*, 2013, **42,** 321–325.

9 R. Q. Nie, X. J. Bo, H. Wang, L. J. Zeng and L. P. Guo, *Electrochemistry Communications*,

2013, **27,** 112–115.

10 Y. X. Tao, J. Y. Dai, Y. Kong and Y. Sha, *Analytical Chemistry*, 2014, **86,** 2633−2639.

11 Y. L. Wei, S. F. Wang, S. M. Shuang and C. Dong, *Talanta*, 2010, **81,** 1800–1805.

12 Y. Kong, J. X. Wei, W. C. Wang and Z. D. Chen, *Electrochimica Acta*, 2011, **56,** 4770–4774.

13 W. D. Laurentis, L. Khim, J. L. R. Anderson,| A. Adam, R. S. Phillips, S. K. Chapman,| K. H. van Pee and J. H. Naismith, *Biochemistry*, 2007, **46,** 12393-12404.

14 H. F. Javier, P. Laporta, F. Gutiérrez, M. D. Rubianes, G. Rivas and M. Martínez, *Electrochemistry Communications*, 2014, **39,** 26–29.

15 C. L. Sun, H. H. Lee, J. M. Yang and C. C. Wu, *Biosensors and Bioelectronics*, 2011, **26,** 3450–3455.

16 J. H. Deng, M. L. Liu, F. B. Lin, Y. Y. Zhang, Y. Liu and S.Z. Yao, *Analytica Chimica Acta*, 2013, **767,** 59–65.

17 L. Wu, L. Y. Feng, J. S. Ren and X. G. Qu, *Biosensors and Bioelectronics*, 2012, **34,** 57–62.

18 E. Asadian, S. Shahrokhian, A. I. zad and E. Jokar, *Sensors and Actuators B*, 2014, **196,** 582–588.

19 X. Q. Ji, L. Cui, Y. H. Xu and J. Q. Liu, *Composites Science and Technology*, 2015, **106**, 25–31.

20 N. An, F. H. Zhang, Z. A. Hu, Z. M. Li, L. Li, Y. Y. Yang, B. S. Guo and Z. Q. Lei, *RSC Advance*, 2015, **5**, 23942–23951.

21 Z. L. Mo, H. Gou, J. X. He, P. P. Yang, C. Feng and R. B. Guo, *Applied Surface Science*, 2012, **258,** 8623–8628.

22 Q. Chen, J. Zhou, Q. Han, Y. H. Wang and Y. Z. Fu, *Colloids and Surfaces B: Biointerfaces*, 2012, **92,** 130–135.

23 Q. Zhang, L. J. Guo, Y. H. Huang, Y. H. Wang, Q. Han and Y. Z. Fu, *Analytical Methods*, 2013, **5,** 4397–4401.

24 L. J. Guo, Q. Zhang, Y. H. Huang, Q. Han, Y. H. Wang and Y. Z. Fu, *Bioelectrochemistry*, 2013, **94,** 87–93.

Figure captions

Scheme 1. Schematic diagram of RGO/PhenCu/GCE synthesis and the electrochemical response of the developed electrode interacting with Trp enantiomers.

Fig. 1. FT-IR spectra of (a) the 1,10-phenanthroline, (b) the 1,10-phenanthroline copper(II), (c) the graphene, and (d) the RGO/PhenCu composites.

Fig. 2. The composition and morphology of (a) the graphene, (b) and (c) the RGO/PhenCu, (d) the PhenCu.

Fig. 3. (a) Cyclic voltammograms of SCE, RGO/PhenCu composites, and after the composites interacted with L-Trp or D-Trp. (b) galvanostatic charge/discharge curves of RGO/PhenCu composites. (c) Cyclic voltammograms after 200 cycles of RGO/PhenCu composites.

Fig. 4. (a) Cyclic voltammograms of RGO/PhenCu composites interacted with D-Trp at different concentrations. (b) Cyclic voltammograms of RGO/PhenCu composites interacted with L-Trp at different concentrations. (c) $\Delta I'$ at different concentrations.

Fig. 5. Time dependence of the discriminating interaction was investigated by cyclic voltammetry. (a) RGO/PhenCu/GCE interacted with L-Trp, (b) the larger image of (a). (c) RGO/PhenCu/GCE interacted with D-Trp, (d) the larger image of (c).

Fig. 6. The influence of pH to the enantioselective discrimination.

Fig. 7. The linear calibration curve for the percentage of L-Trp. Inset: the larger image of cyclic voltammograms of Trp enantiomeric mixtures.

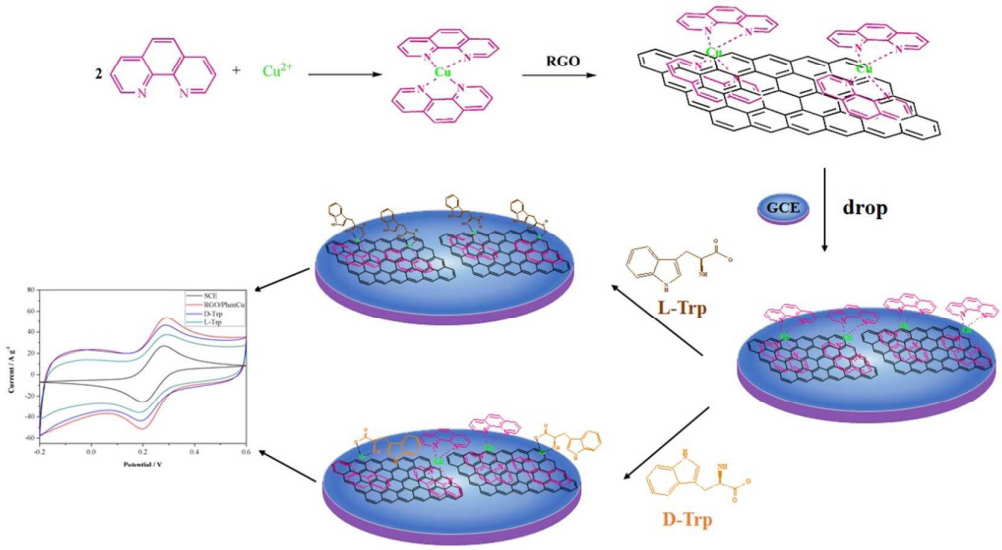

Scheme 1

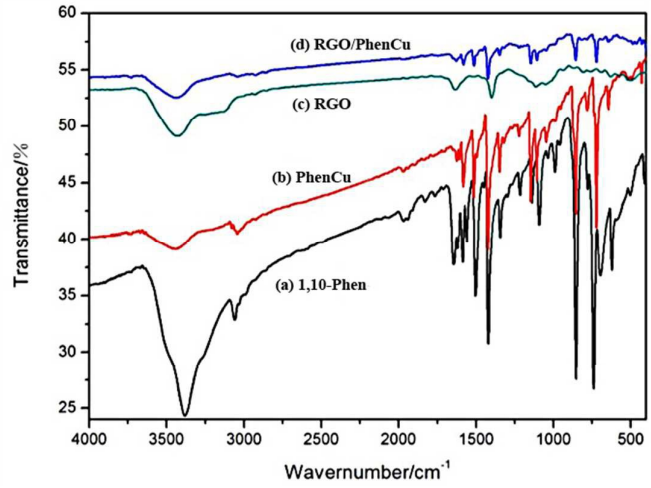

Fig. 1

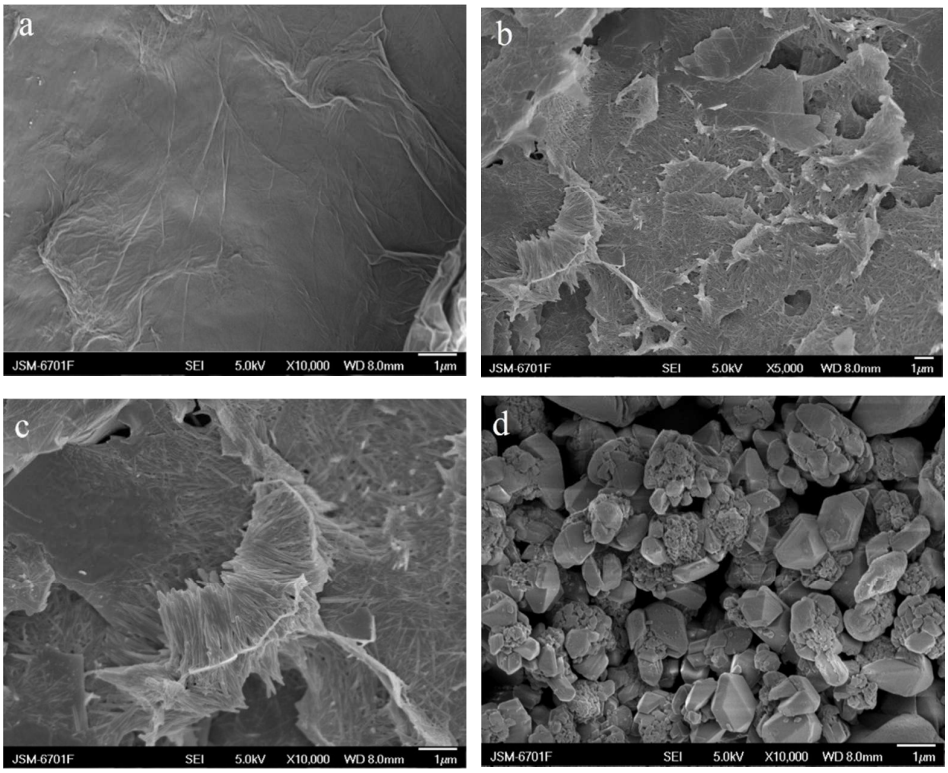

Fig. 2

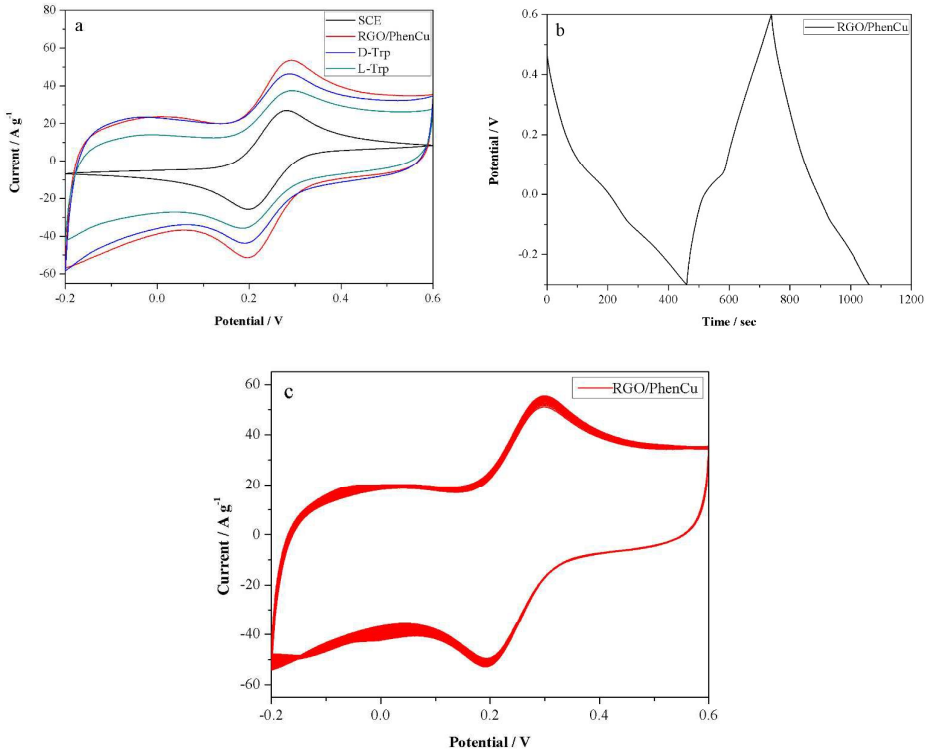

Fig. 3

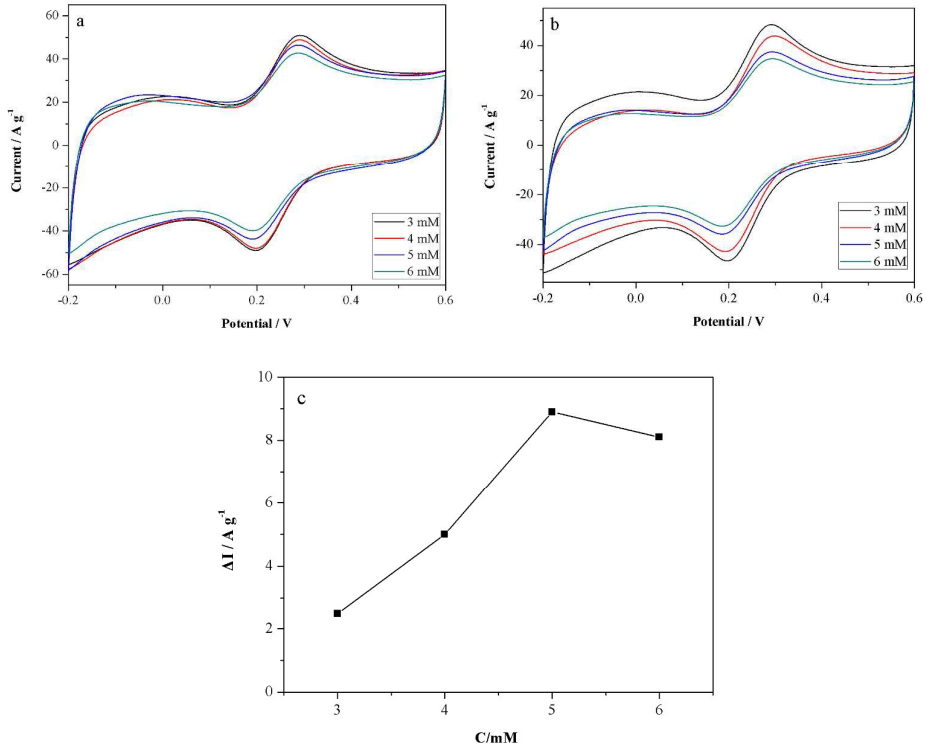

Fig. 4

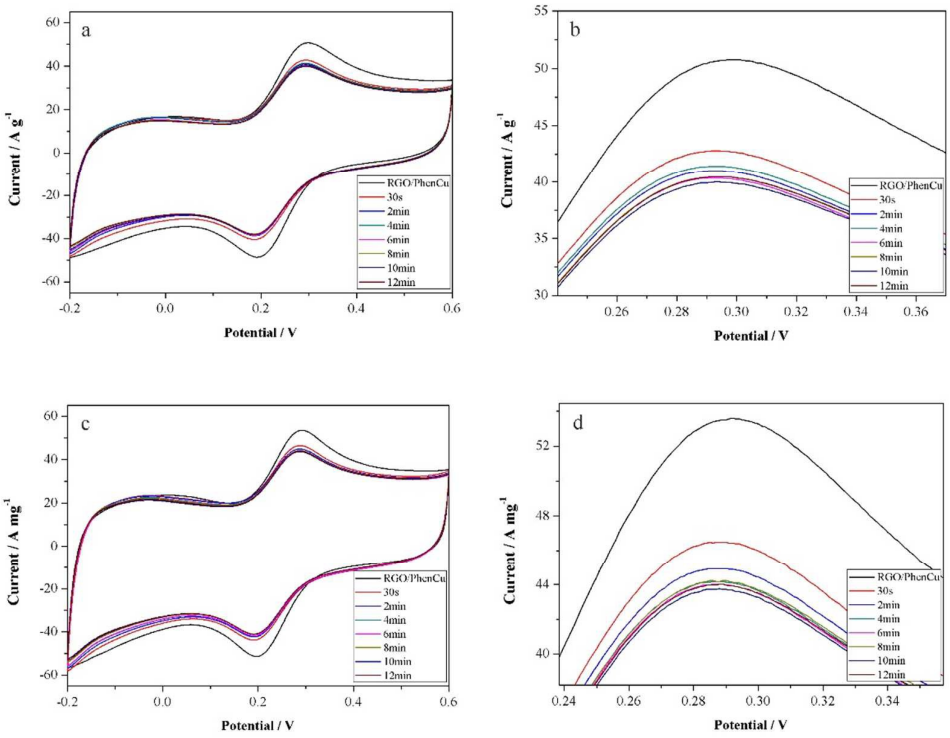

Fig. 5

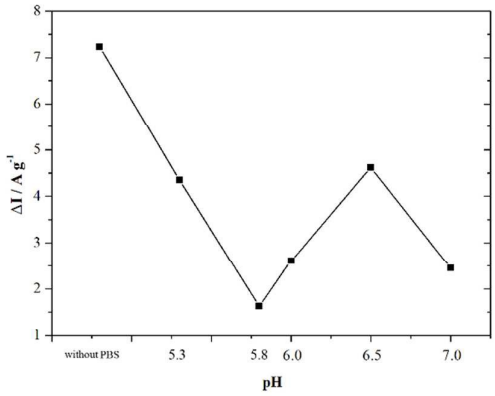

Fig. 6

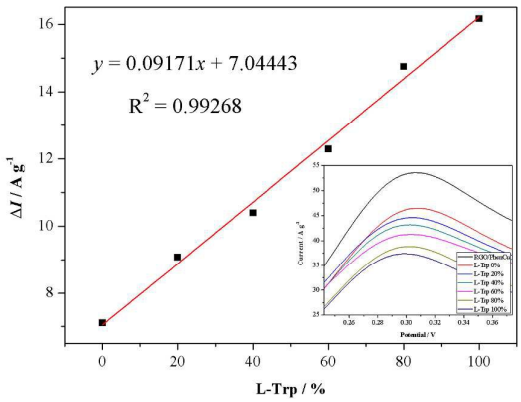

Fig. 7

Table 1 Comparison of electrochemical chiral sensor of tryptophan enantiomers

Ref.	chiral recognition materials	interaction time	pH	R^2
8	ITO/APTES/GO/HSA	—	7.01	0.986
22	l-Cys-Au	15 min	5.4	0.9937
23	HSA/MB–MWNT	15 min	7.4	0.9828
24	ds-DNA/THi–GR	20 min	5.5	0.9959
This work	RGO/PhenCu	6 min	Without adjustment	0.9927

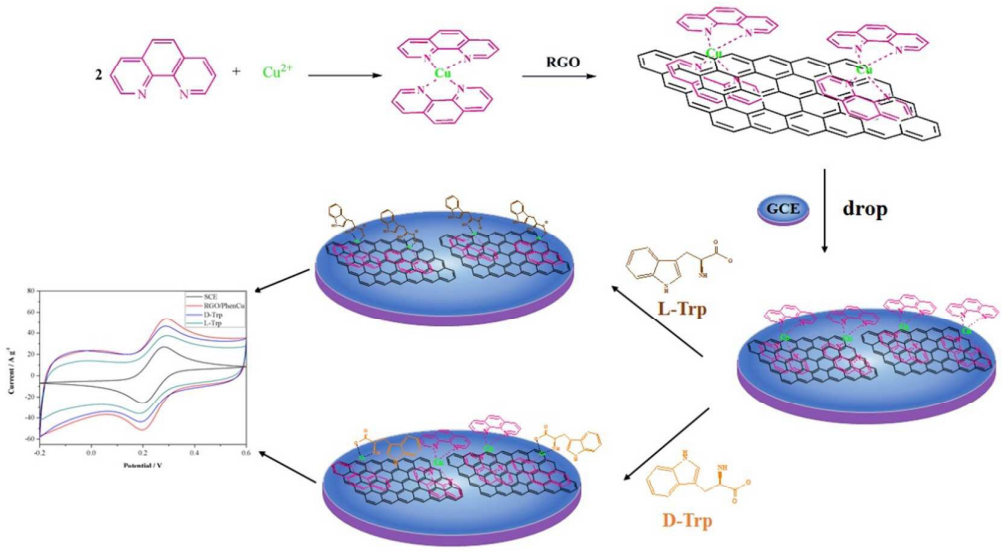

Graphical abstract